Seasonal and Long-Term Trends in Land Cover Transformation and Urban Microclimate in Dhaka and Chittagong

Md. Farid Uddin[1], Mohammad Shahidul Islam[1] , Fatema Afnan Chowdhury[1], Md. Mahadi Hasan Seyam[1], Adib Mahmud[1] , Ishpiya Mahreen Chowdhury[1]

Bangladesh Space Research and Remote Sensing Organization (SPARRSO),
Agargaon, Sher-e-Bangla Nagar, Dhaka-1207, Bangladesh

DOI: 10.29322/IJSRP.16.06.2026.p17423
https://dx.doi.org/10.29322/IJSRP.16.06.2026.p17423

Paper Received Date: 5th May 2026
Paper Acceptance Date: 24th June 2026
Paper Publication Date: 28th June 2026

Abstract- Urbanization and changes in land use significantly impact vegetation patterns, land surface temperature (LST), and urban heat island (UHI) effects. This study uses multi-temporal satellite images from 2000 to 2025 to examine seasonal and long-term land use and land cover (LULC) changes in Dhaka and Chittagong, Bangladesh. It also looks at derived indices such as NDVI, LST, UHI, and UTFVI profiles. The findings show considerable urban growth over the 25-year period. In Chittagong, built-up areas grew by 47.82% to 53.88% across different seasons, leading to a marked reduction in agricultural land and barren fields. Dhaka showed an even more aggressive trend, with built-up areas nearly doubling by taking over croplands and wetlands. NDVI metrics reveal increased spatial fragmentation and serious vegetation loss within urban centers, even though there was some localized recovery during the monsoon. Thermal assessments indicate a steady rise in LST. From 2000 to 2025, peak monsoon LST increased from 36.06°C to 39.81°C in Chittagong and from 32.61°C to 39.56°C in Dhaka. At the same time, maximum UHI intensities grew, reaching 3.51°C in Chittagong and about 3.0°C in Dhaka, mainly during the monsoon. Overall, these results establish a strong link between rapid urban expansion and increased thermal stress on microclimates, providing important insights for climate-resilient urban planning in Bangladesh.

Index Terms- Land Use/Land Cover (LULC), NDVI, Land Surface Temperature (LST), Urban Heat Island (UHI), Remote Sensing, Urbanization

I.INTRODUCTION

Urbanization is one of the most pervasive and consequential land-use transformations of the twenty-first century. Between 2000 and 2020, global urban land cover expanded by approximately 80,000 km², and the United Nations projects that nearly 70% of the world's population will reside in urban areas by 2050 (UN-Habitat, 2022). This rapid spatial growth fundamentally alters the land surface energy balance: impervious surfaces replace permeable soils and vegetation, reducing latent heat flux and amplifying sensible heat exchange, thereby elevating land surface temperature (LST) and intensifying the urban heat island (UHI) effect (Oke, 1982; Zhao et al., 2014). The cascading consequences—increased energy demand, heat-related mortality, deteriorating air quality, and disrupted hydrological cycles—are disproportionately severe in rapidly growing cities of South and Southeast Asia, where institutional capacity to manage urban growth often lags behind demographic pressure (Patz et al., 2005; Grimm et al., 2008).

Land use/land cover (LULC) change is the primary driver of urban thermal dynamics. Conversion of agricultural land, wetlands, and natural vegetation to built-up surfaces reduces the Normalized Difference Vegetation Index (NDVI), diminishes evapotranspiration cooling, and increases surface albedo variability in ways that amplify LST (Weng et al., 2004; Li et al., 2011; Zhou et al., 2014). Conversely, urban green spaces—parks, tree canopies, and riparian corridors—demonstrably attenuate UHI intensity through shading and latent heat dissipation (Cao et al., 2010; Bowler et al., 2010). The interplay between built-up expansion, vegetation loss, and surface heating is therefore nonlinear and season-dependent: monsoon-driven leaf-out can temporarily counteract thermal stress even in heavily urbanized environments, while pre-monsoon transition periods exhibit peak LST when solar radiation is maximum and soil moisture is minimal (Islam et al., 2019; Amani et al., 2020). Disentangling these seasonal dynamics is essential for designing thermally resilient urban landscapes.

Multi-temporal satellite remote sensing provides the only practical means of monitoring LULC and LST changes at city scale across multi-decadal time horizons. The Landsat programmed—spanning Landsat 5 Thematic Mapper (TM), Landsat 8 Operational Land Imager/Thermal Infrared Sensor (OLI/TIRS), and Landsat 9—offers an unbroken archive of 30-m optical and 100-m (resampled to 30-m) thermal imagery since 1984, making it the instrument of choice for decadal LULC–LST assessments (Wulder et al., 2022). Sentinel-2 Multispectral Instrument (MSI) imagery, with its 10-m spatial resolution and five-day revisit cycle, further enhances the spatial detail achievable for recent classification epochs (Drusch et al., 2012). Cloud computing platforms—particularly Google Earth Engine (GEE)—have democratized access to these archives and enabled the computation of spectral indices such as NDVI, Normalized Difference Built-up Index (NDBI), Normalized Difference Water Index (NDWI), and Bare Soil Index (BSI) at continental scale, while machine learning classifiers such as Random Forest (RF) have substantially improved LULC mapping accuracy over traditional maximum-likelihood approaches (Gorelick et al., 2017; Belgiu & Drăguţ, 2016).

LST retrieval from Landsat thermal data using NDVI-based emissivity correction is a well-established and reproducible procedure (Sobrino et al., 2004; Avdan & Jovanovska, 2016). Beyond LST, the UHI intensity index—defined relative to the spatial mean and standard deviation of LST within the study area—provides a dimensionless, scene-invariant metric that facilitates inter-year and inter-city comparisons (Weng, 2009). The Urban Thermal Field Variance Index (UTFVI) complements UHI analysis by classifying thermal environmental quality into ordinal ecological condition categories, thereby translating continuous LST fields into policy-relevant heat stress zones (Chen et al., 2006; He et al., 2011). Integrating LULC change detection with NDVI, LST, UHI, and UTFVI within a unified spatiotemporal framework enables a comprehensive diagnosis of urban thermal degradation.

Bangladesh presents one of the world's most acute cases of rapid, unplanned urban expansion. Dhaka, the capital and primate city, has grown from approximately 2 million inhabitants in 1975 to over 21 million in 2023, making it one of the ten most densely populated metropolitan areas globally (World Bank, 2023). Chittagong (Chattogram), the principal seaport and industrial hub, has undergone equally transformative growth driven by export-oriented manufacturing, port development, and rural-to-urban migration. Previous remote sensing studies of Bangladesh's urban cores have documented rising LST and UHI intensity in response to built-up expansion in Dhaka (Rana et al., 2021; Hasan et al., 2023) and Chittagong (Iqbal & Khan, 2014; Islam et al., 2021). However, most existing studies are limited to a single city, a single season, or fewer than three-time epochs, constraining the ability to characterize intra-annual thermal variability or to track long-term trajectories across structurally different urban morphologies.

A systematic, multi-decadal, multi-seasonal comparison of LULC dynamics and their thermal environmental consequences across both Dhaka and Chittagong districts is absent from the literature. Existing assessments rarely extend to 2025, precluding analysis of the most recent phase of urban expansion accelerated by post-COVID infrastructure projects and continued rural in-migration. Furthermore, the seasonal decomposition of LST and UHI signals across winter (November–February), transition (March–June), and monsoon (July–October) seasons has not been systematically examined for these districts, despite the profound influence of Bangladesh's monsoonal climate on surface energy partitioning and vegetation phenology. Without this seasonal lens, urban heat stress assessments risk conflating climatological seasonality with anthropogenic land-cover change signals.

The present study addresses these gaps through a 25-year (2000–2025) spatiotemporal assessment of Dhaka and Chittagong districts using multi-sensor Landsat and Sentinel-2 imagery processed within the GEE cloud computing environment. The specific objectives are: (i) to map and quantify seasonal and long-term LULC changes across five land-cover classes; (ii) to characterize spatial and temporal dynamics of NDVI as an indicator of vegetation condition; (iii) to retrieve and analyse seasonal LST patterns and their response to LULC transformation; (iv) to assess UHI intensity and UTFVI-based ecological quality across seasons and years; and (v) to synthesize the relationships among urban growth, vegetation degradation, and surface thermal stress to inform climate-resilient land-use planning in rapidly urbanizing Bangladesh.

The findings of this study contribute to the growing body of literature on urban environmental change in South Asia and provide empirically grounded evidence for urban heat mitigation strategies in Bangladesh. By integrating long-term LULC trajectories with seasonal thermal diagnostics across two morphologically distinct districts, the study offers a replicable methodological template for comparable assessments across the rapidly urbanizing Global South. The results are directly relevant to Bangladesh's National Adaptation Plan, the Climate Change Master Plan for Dhaka Metropolitan Area, and Chittagong's Urban Development Plan, each of which identifies thermal comfort, green infrastructure, and sustainable land use as priority intervention domains.

II. METHODOLOGY

Figure 1 shows the methodological approach of this study, which used an integrated approach of remote sensing and geospatial analysis to find out the spatiotemporal variation of land use/land cover (LULC),
vegetation condition, land surface temperature (LST), urban heat island (UHI) and urban thermal field variance index (UTFVI) in Dhaka and Chittagong for the period 2000 to 2025. Landsat 5, Landsat 8/9 and Sentinel-2 data were used to create seasonal composites for winter (November to February), transition (March to June), and monsoon (July to October). Cloud masking and preprocessing were conducted followed by various spectral indices such as NDVI, NDBI, NDWI and BSI which were derived and subsequently classified

using Random Forest (RF) supervised classification technique. The NDVI was also used to calculate fractional vegetation cover and land surface emissivity to calculate LST from thermal imagery. After the LST outputs, the urban thermal characteristics and ecological conditions

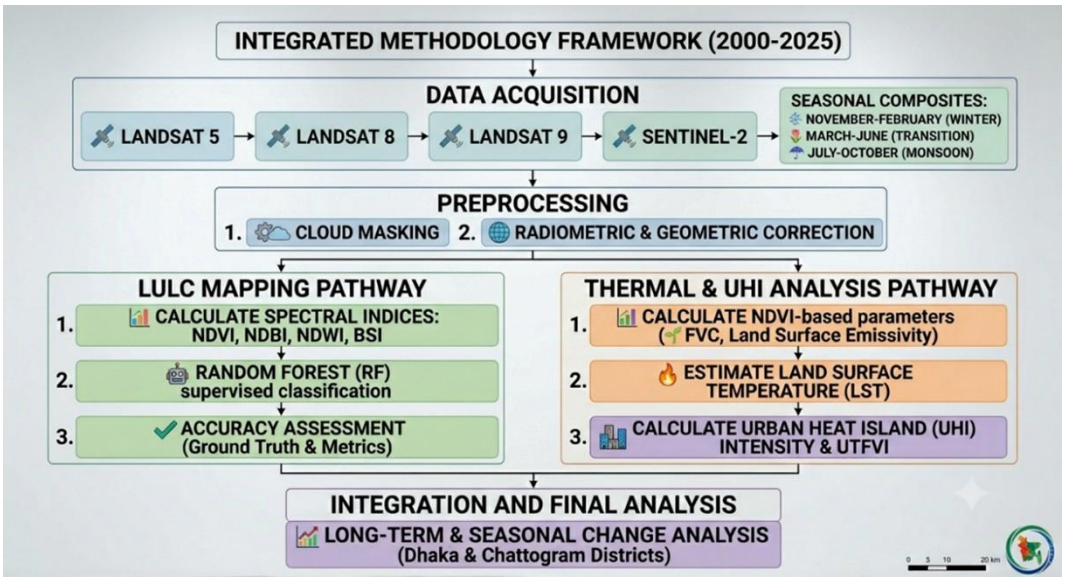

Figure 1: Overall methodological framework for the study

were assessed through the calculation of UHI intensity and UTFVI. Lastly, the created LULC, NDVI, LST, UHI, and UTFVI maps were analyzed to explore the environmental changes that have taken place over the long term (2000–2025) and seasons in the study areas.

A. Study Area

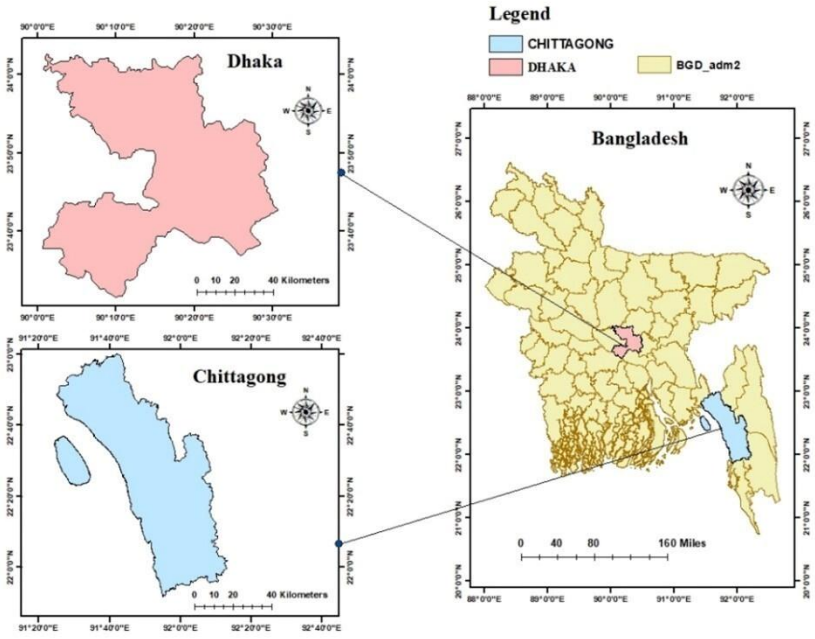

FIGURE 2: STUDY AREA MAP

The study took place in the two major and most economically significant cities of Bangladesh, namely **Figure 2.** Dhaka and Chittagong. The capital city Dhaka is very densely populated, with a very fast urbanization rate, and intensive infrastructural development. Chittagong is the main port of Bangladesh, a city that has seen significant urbanization over the last few decades, is important to national trade and industrial activity. The selection of these cities was based on their fast changes in land use and the growing awareness of thermal environmental degradation in cities.

B. Data Collection

To evaluate land use/land cover (LULC) change, vegetation dynamics, land surface temperature (LST), urban heat island (UHI), and urban thermal field variance index (UTFVI) over the period from 2000 to 2025, multi-temporal satellite images from Landsat and Sentinel missions were used. The Google Earth Engine (GEE) cloud computing platform was used for all image processing and analyses. The study year was divided into three climatic seasons to investigate seasonal variability. Such as: Winter: November–February, Transition: March–June and Monsoon: July–October. Four representative years (2000, 2010, 2020, and 2025) were selected for analysis. The satellite data sets and analysis years used for mapping Land Use/Land Cover (LULC), Normalized Difference Vegetation Index (NDVI) and Land Surface Temperature (LST) are illustrated in **Table 1**.

Table 1: Satellite datasets used in the study

Analysis	Year	Satellite
LULC	2000, 2010	Landsat 5 TM
	2020, 2025	Sentinel-2 MSI
NDVI	2000, 2010	Landsat 5 TM
	2020	Landsat 8 OLI
	2025	Landsat 8/9 OLI
LST	2000, 2010	Landsat 5 TM
	2020	Landsat 8 OLI/TIRS
	2025	Landsat 8/9 OLI/TIRS

C. Image Preprocessing

All acquired satellite images were preprocessed to high quality with pixel-based analysis in the Google Earth Engine (GEE) cloud computing platform. One of the most important steps was the removal of contaminated and shadowed pixels caused by cloud for each pixel in the image based on the Quality Assessment (QA) bands defined for each satellite sensor, such as the QA_PIXEL band for Landsat and the QA60 band for Sentinel-2.

After pixel clearing, seasonal composite images have been produced. This was done by using a median-reducing function of all cloud-free observations in the seasons of interest, which helped minimize seasonal phenological variations or sensor artifacts. Lastly, the resulting seamless composite mosaics were cropped to the exact administrative boundaries of Dhaka and Chittagong and the administrative-defined region of interest (ROI) for subsequent spatial analysis was identified.

D. Land Use/Land Cover Classification

The supervised classification approach was applied to land use/land cover (LULC) mapping in GEE. A classification scheme comprised of five mutually exclusive major LULC classes in **Table 2** was developed for the study areas based on the geographical characteristics of each of the study areas.

Table 2: Description of the classification area

SI No.	Class	Description
1	Urban/Built-up Land	Areas of residential, commercial, industrial activity, transport infrastructure and paved surfaces.
2	Agricultural land	Active crop fields, fallow agricultural land, and prepared farming plots.
3	Vegetation	Dense forests, orchards, parks, shrubs and natural green cover.
4	Water Bodies	Rivers, ponds (aquaculture), permanent canals, lakes and wetlands.
5	Bare Land	Exposed soil, sandbars (char lands), construction sites, and uncultivated vacant plots.

A large number of training samples was obtained through visual interpretation of high-resolution historical Google Earth imagery and time-series spectral profiles to train the classifier. The data was split 70% to train the supervised machine learning classifier (e.g., Random Forest) and 30% was kept aside for independent validation. Finally, the trained algorithm was used on the seasonal composites to produce thematic maps of LULC. To eliminate noise, post-classification smoothing was applied, and to assess the accuracy of the final maps, the Overall Accuracy and the Kappa coefficient were calculated against ground truth maps by means of the confusion matrix.

E. NDVI Calculation

The Normalized Difference Vegetation Index (NDVI) was calculated for each study period to monitor vegetation density and health dynamics using Equation 1

$$NDVI = \frac{NIR - Red}{NIR + Red} \quad (1)$$

where **NIR** represents near-infrared reflectance and **Red** represents red-band reflectance. NDVI values range from −1 to +1, with higher positive values indicating denser and healthier vegetation.

Land Surface Temperature (LST) Retrieval

Land Surface Temperature (LST) was extracted from Landsat thermal data with the emissivity correction method based on the NDVI. The proportion of vegetation (Pv) was first estimated using the red and near-infrared bands, with maximum and minimum NDVI values to determine the percentage of vegetation. The percentage of vegetation was estimated from the NDVI values with Equation 2

$$P_v = \left(\frac{NDVI - NDVI_{min}}{NDVI_{max} - NDVI_{min}}\right)^2 \quad (2)$$

where $NDVI_{min}$ and $NDVI_{max}$ represent the minimum and maximum NDVI values within the study area.
Afterward, land surface emissivity (ε) was derived from P_v to reflect the land surface characteristics. The estimation of surface emissivity was performed based on the vegetation proportion by using Equation 3

$$\varepsilon = 0.004P_v + 0.986 \quad (3)$$

In this approach, it is assumed that emissivity increases with vegetation density and is commonly used in NDVI-based LST retrieval studies.
For Landsat 8/9 OLI-TIRS imagery (2020 and 2025), brightness temperature was obtained from the surface temperature band (ST_B10) using the scaling factor provided in Equation 4

$$BT = (ST_{B10} \times 0.00341802) + 149.0 \quad (4)$$

where 0.00341802 is the multiplicative scale factor and 149.0 is an additive offset. Similarly, for Landsat 5 TM imagery (2000 and 2010), brightness temperature was derived from the thermal band (Band 6) using Equation 4, with only the band-specific input replaced accordingly.
Finally, emissivity-corrected land surface temperature was calculated for both Landsat 5 and Landsat 8/9 datasets using Equation 5:

$$LST = \frac{BT}{1 + \left(\frac{\lambda \cdot BT}{\rho}\right)\ln(\varepsilon)} - 273.15 \quad (5)$$

where:

- ***LST*** = Land Surface Temperature (°C)
- ***BT*** = Brightness Temperature (K)
- λ = wavelength of emitted radiance
- ρ = 1.438×10^{-2} m K
- ε = land surface emissivity

The final LST maps were generated for all years and seasons to evaluate thermal variability across the study areas.

F. Urban Heat Island (UHI) Analysis

The intensity of the Urban Heat Island (UHI) phenomenon was deduced from the generated Land Surface Temperature (LST) maps. Regions that demonstrated elevated thermal readings in comparison to the adjacent landscape were recognized as urban heat island zones. UHI maps were developed for each specific year and season to evaluate the consequences of urban expansion on thermal conditions.

The UHI index was calculated by using Equation (6)

$$UHI = \frac{LST - LST_{mean}}{SD} \quad (6)$$

where:

- LST = pixel-wise land surface temperature
- LST_{mean} = mean land surface temperature of the study area
- SD = standard deviation of land surface temperature

Urban Thermal Field Variance Index (UTFVI)

The Urban Thermal Field Variability Index (UTFVI) was utilized to evaluate urban ecological quality and thermal environmental conditions. The Index was computed by using Equation (7)

$$UTFVI = \frac{LST - LST_{mean}}{LST_{mean}} \quad (7)$$

where:

- LST = pixel-wise land surface temperature
- LST_{mean} = mean land surface temperature of the study area

Elevated UTFVI values signify heightened thermal stress and diminished ecological conditions, while reduced values suggest more advantageous environmental quality. According to the UTFVI assessments, the study area was categorized into six ecological evaluation classes, ranging from Strongest to None in **Table 3** in terms of thermal environmental conditions.

Table 3: Threshold UTFVI value for ecological evaluation and thermal comfort.

UTFVI range	UHI presence	Ecological evaluation index
<0	None	Excellent
0–0.005	Weak	Good
0.005–0.010	Middle	Normal
0.010–0.015	Strong	Bad
0.015–0.020	Stronger	Worse
>0.020	Strongest	Worst

G. Change Detection and Comparative Analysis

Longitudinal analyses concentrated on identifying transformations between the years 2000 and 2025, whereas seasonal analyses scrutinized intra-annual fluctuations in land cover configurations, vegetative dynamics, surface temperature, UHI intensity, and ecological thermal conditions. The interrelationships among urban expansion, vegetative alterations, and thermal environmental indicators were subsequently examined to evaluate the implications of urbanization on environmental quality in the cities of Dhaka and Chittagong.

III. RESULT AND DISCUSSION

A. Spatiotemporal and Seasonal Dynamics of LULC in Chittagong (2000–2025)

Chittagong saw significant land cover change from 2000 to 2025 in **Figure 3**, with a notable increase in urban areas and water bodies. Urban land rose by 47.82% from 328.46 km² to 485.52 km² during the winter season. The expansion of residential, commercial, industrial and port-related infrastructure is also reflected in similar increases during the transition (48.54%) and monsoon (53.88%) seasons. The water bodies also grew significantly in all seasons, especially the winter season, with a growth of 70%, which is likely related to aquaculture development, coastal water retention areas, and hydrological changes. Agricultural land, on the other hand, saw a decrease of 6.20% in the winter season, and the amount of bare land reduced significantly in every season. The vegetation cover in the district was found to be relatively stable with minor reduction during winter (-2.62%) and monsoon (-6.72%); this implies that there are still forested and hilly areas of the district which cover up a considerable portion of the area despite the continuous urbanization.

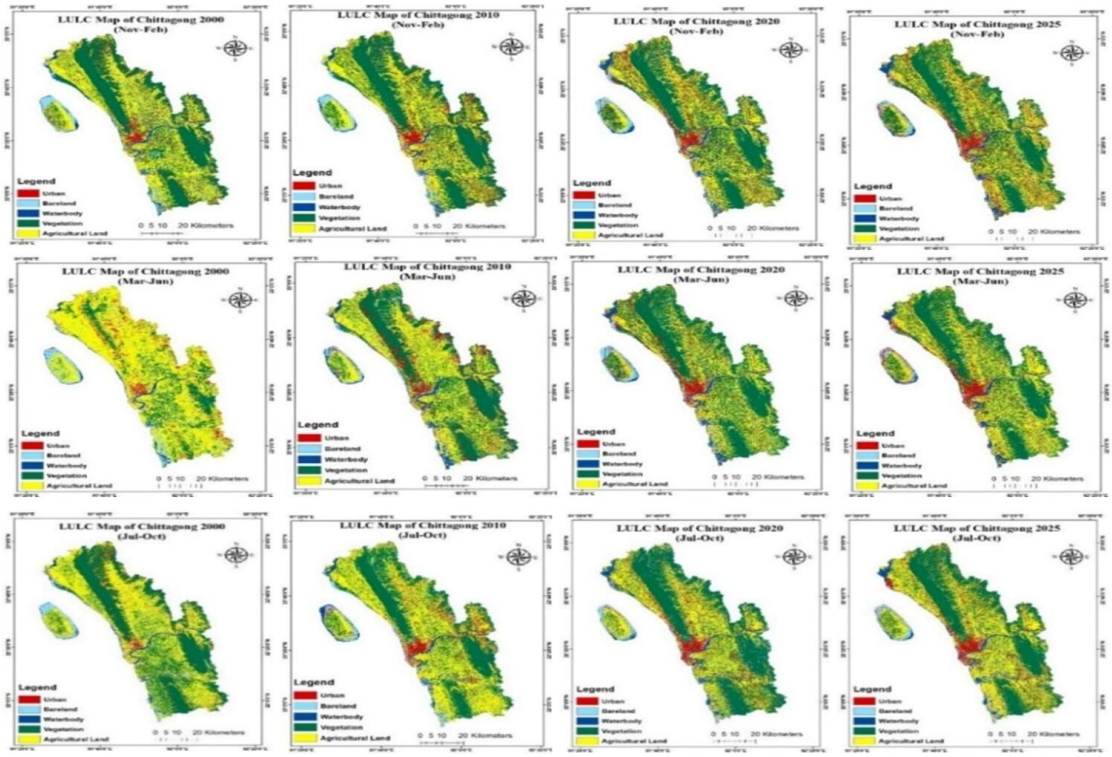

Figure 3: LULC Map of Chittagong during the Winter (Nov-Feb), Transition (Mar-Jun), Monsoon (Jul-Oct) Period (2000,2010,2020 & 2025)

There is a seasonal variation in Chittagong in **Figure 4** for all the LULC classes. The vegetation cover was maximum during the transition season from 1492.70 km² in 2000 to 2001.11 km² in 2025. This increase is probably due to favorable climatic conditions prevailing before the onset of the monsoon, such as the rise in temperature and rainfall which favor vegetation growth. The agricultural land area seemed to be at its peak in the monsoon with the highest extent of 1649.92 km² in 2025, as rain-fed agriculture is prevalent and Aman rice is grown widely. More surface water was also present during the monsoon and transition seasons, also when the precipitation was heavier. Urban areas were predominant throughout the year with the highest urbanization in the winter season.

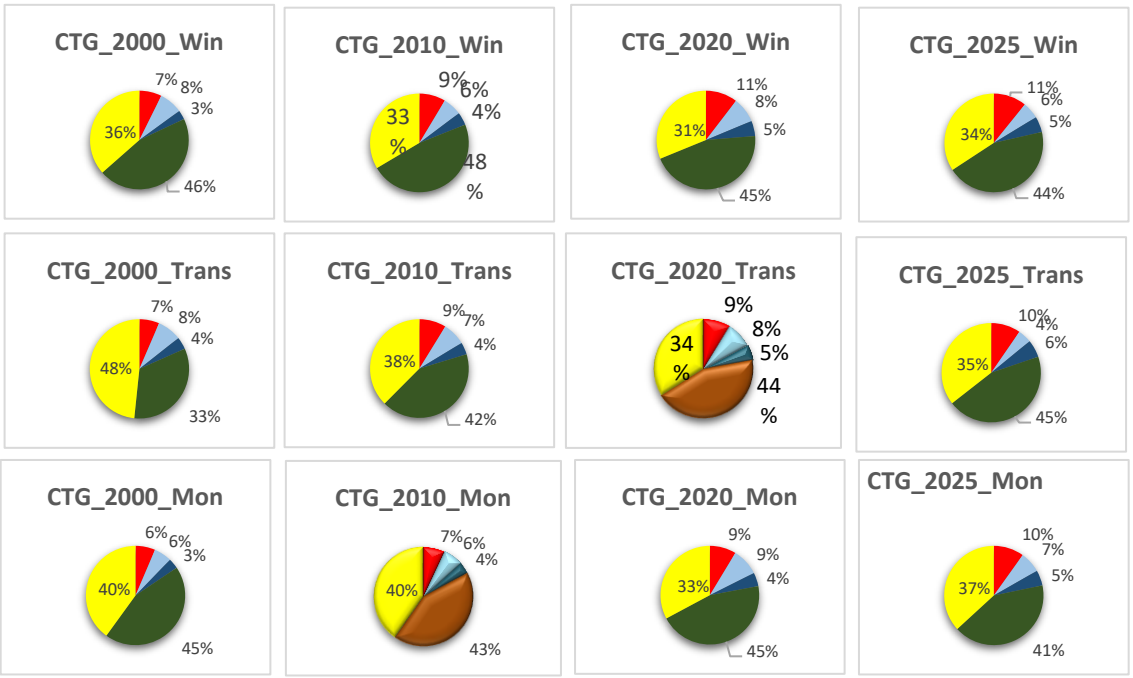

Figure 4: Percentage Distribution of Land Use/Land Cover Classes in Chattogram During Winter, Transition and Monsoon Seasons (2000–2025)

B. Spatiotemporal and Seasonal Dynamics of LULC in Dhaka (2000–2025)

Dhaka was found to be the area with the most marked urbanization among the study areas. Urban land increased in **Figure 5** from 180.11 km² to 372.56 km² during winter (+106.86%), from 192.96 km² to 385.35 km² during the transition season (+99.71%), and from 182.49 km² to 370.55 km² during the monsoon season (+103.05%). This quick growth can be interpreted as being related to high population growth, infrastructure development, industrialization and outward growth of the metropolitan region. Agricultural land, on the other hand, saw a reduction of 24.90%, 30.91% and 21.83% in the winter, transition and monsoon periods, respectively, suggesting the encroachment of built-up areas onto agricultural land. Overall, the water bodies experienced moderate decreases in the winter (-10.2%) and the monsoon (-24.82%), whereas the vegetation observed moderate increases in the winter and transition and relatively stable overall. The loss of bare ground in most seasons is also indicative of a high degree of land development and urbanization. The changes in LULC in **Figure 6** Dhaka were relatively small and insignificant because built-up areas dominate the city. During monsoon (2010), highest vegetation cover was observed and during transition season, vegetation cover has been increased from 267.02 km² in 2000 to 300.83 km² in 2025. These patterns are indicative of better growth of vegetation in response to higher rainfall and climatic conditions. Agricultural land was also an important class of land cover throughout the year but was at its maximum in the winter season, with an area of 834.40 km² in 2000.

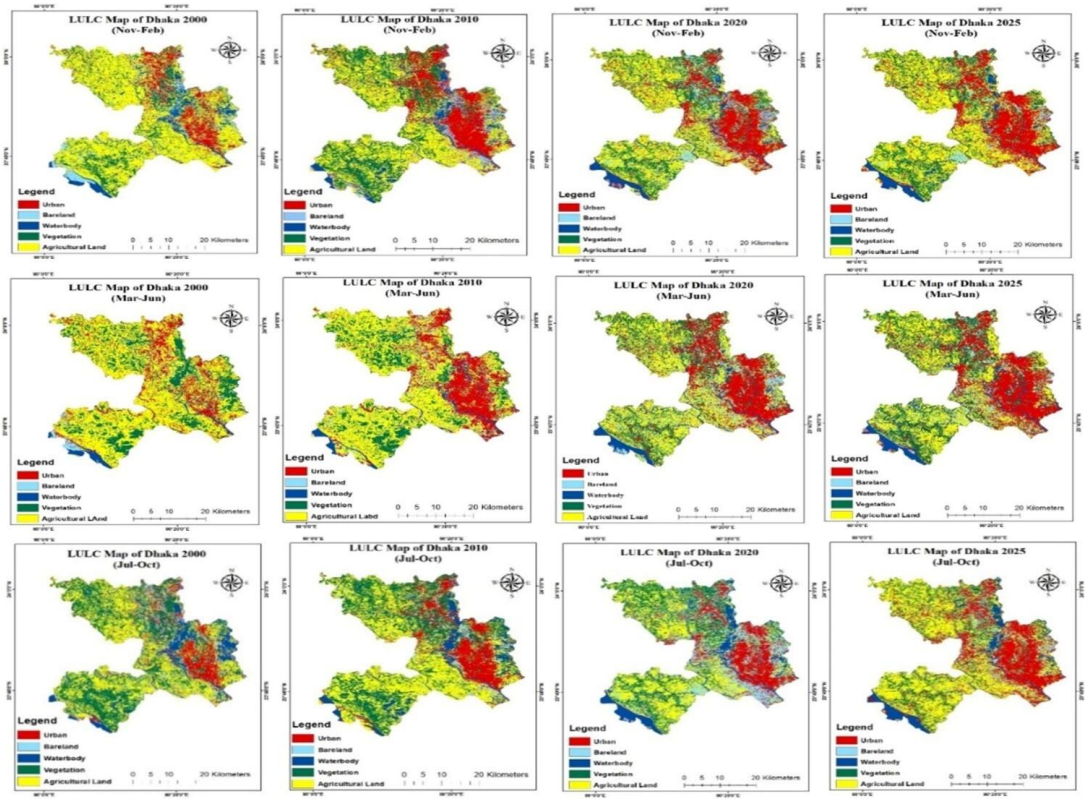

Figure 5: LULC Map of Dhaka during the Winter (Nov-Feb), Transition (Mar-Jun), Monsoon (Jul-Oct) Period (2000,2010,2020 & 2025)

Water bodies showed moderate seasonal variations, greater extent during monsoon season because of seasonal flooding and heavy run-offs during that season. But due to the continuous growth in urban areas, the agricultural as well as aquatic environment is also shrinking gradually in the district.

C. Classification Accuracy Assessment

The Random Forest (RF) classifier showed good classification accuracy for both study areas in all years and seasons. Overall Accuracy (OA) in Chittagong varied from 78% to 90% in **Table 4** and Kappa coefficient from 0.71 to 0.87.

Table 4: Different Years Classification Accuracy for Chittagong

Year	Overall Accuracy (%)	Kappa Coefficient
2000	87-80	0.82-0.74
2010	87-78	0.83-0.71
2020	85-79	0.82-0.73
2025	90-87	0.87-0.83

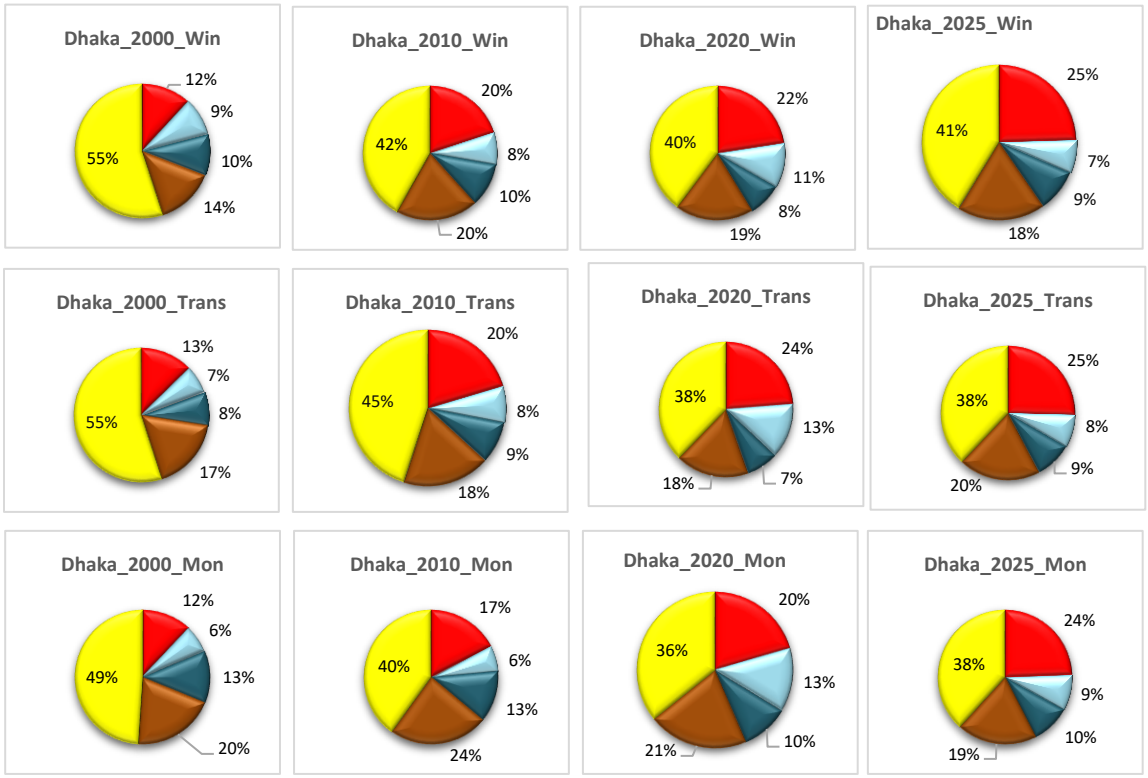

Figure 6: Percentage Distribution of Land Use/Land Cover Classes in Dhaka During Winter, Transition and Monsoon Seasons (2000–2025)

Likewise, in Dhaka, the values of OA were in **Table 5** between 78% and 93%, and the Kappa coefficient was between 0.71 and 0.92. The accuracy metrics show that there is a high to very high level of agreement between the classified maps and the reference samples, which confirms the reliability of the LULC maps generated for subsequent spatiotemporal change analyses. These satisfactory classification results were used to explore the long-term land-cover changes and seasonal variations in Dhaka and Chittagong from 2000 to 2025. The analysis showed that there were significant changes in the spatial distribution of urban, agricultural, vegetation, water, and bare land classes, which were attributed to the effects of rapid urbanization and environmental change. The detailed patterns of these changes are discussed in the above sections.

Table 5: Different Years Classification Accuracy for Dhaka

Year	Overall Accuracy (%)	Kappa Coefficient
2000	90-78	0.87-0.71
2010	87-78	0.83-0.71
2020	90-79	0.87-0.73
2025	93-89	0.92-0.86

D.Spatiotemporal Variations of NDVI, LST, UHI, and UTFVI in Chittagong (2000–2025)

Between 2000 and 2025, Chittagong faced increasing thermal stress even with significant vegetation cover. Forested and vegetated areas remained important parts of the landscape, with maximum NDVI in **Figure 7** rising slightly from 0.488 to 0.497 in winter and from 0.554 to 0.578 during the monsoon. However, temperatures increased sharply. Maximum winter LST in **Figure 8** went up from 33.26°C to 35.31°C, while monsoon LST jumped from 36.06°C to 39.81°C. At the same time, maximum UHI intensity **Figure 9** rose from 2.35°C to 2.58°C in winter and from 3.20°C to 3.51°C in the monsoon.

These environmental changes reflect a 47.82% increase in urban development due to rapid urbanization, industrialization, and port activities. Mapping of the Urban Thermal Field Variance Index (UTFVI) shows in **Figure 10** a steady decline in the thermal environment, highlighting a clear growth of "strong" and "strongest" thermal stress zones. Strong seasonal patterns appeared across all indices. The monsoon season had the highest NDVI values (Figure 7), peaking at 0.578 in 2025, thanks to ample rainfall. In contrast, peak LST happened during the pre-monsoon transition season when solar heating is at its highest and ambient moisture is at its lowest. Ultimately, while seasonal vegetation growth helps lower surface temperatures to some extent, ongoing urban sprawl keeps increasing localized thermal stress.

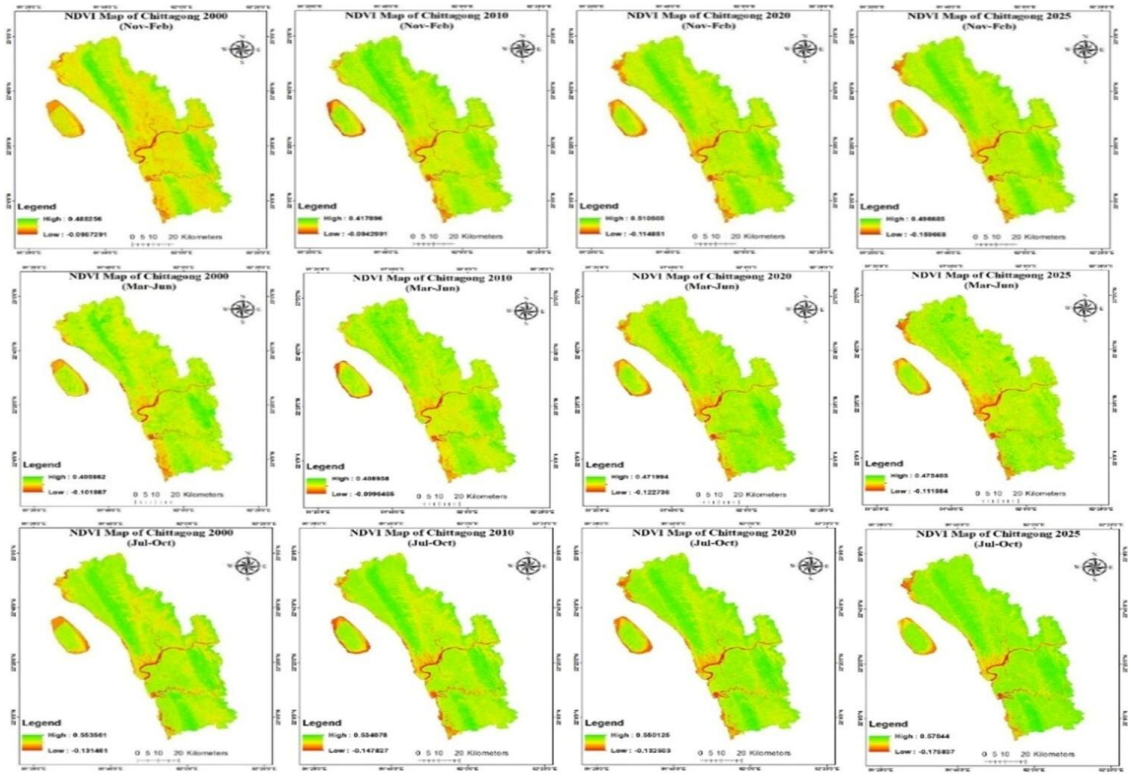

Figure 7: NDVI Map of Chittagong during the Winter (Nov-Feb), Transition (Mar-Jun), Monsoon (Jul-Oct) Period (2000,2010,2020 & 2025)

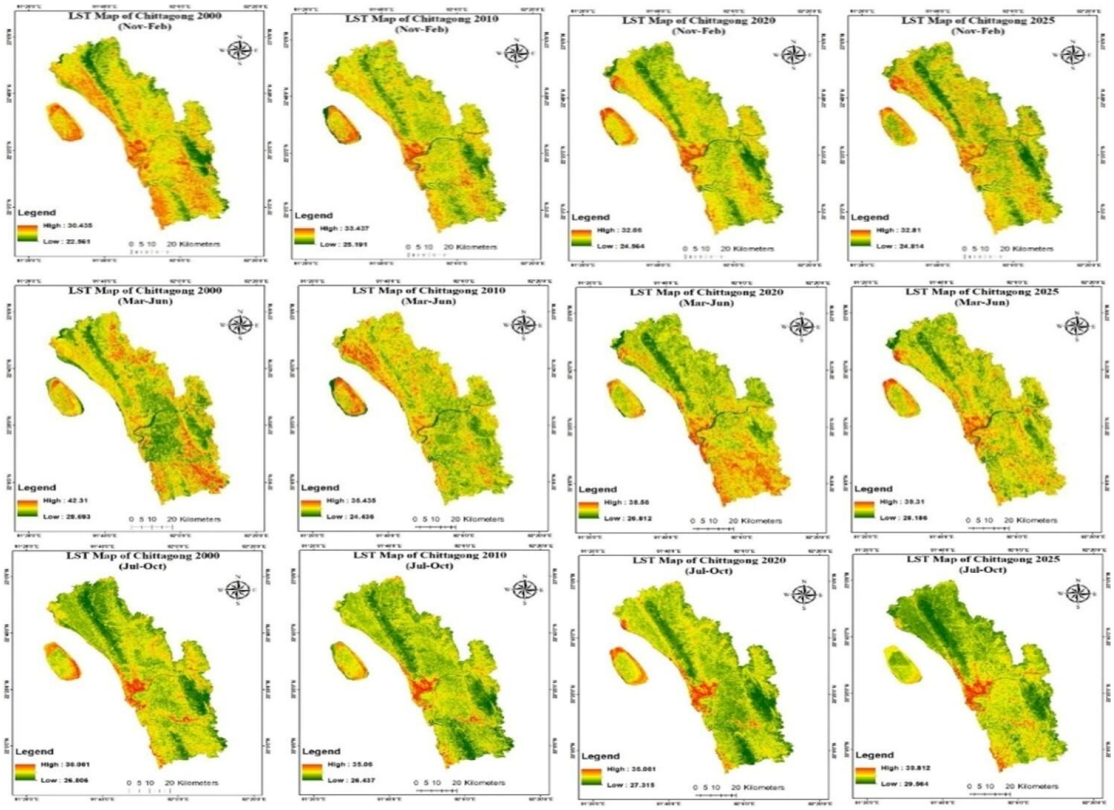

Figure 8: LST Map of Chittagong during the Winter (Nov-Feb), Transition (Mar-Jun), Monsoon (Jul-Oct) Period (2000,2010,2020 & 2025)

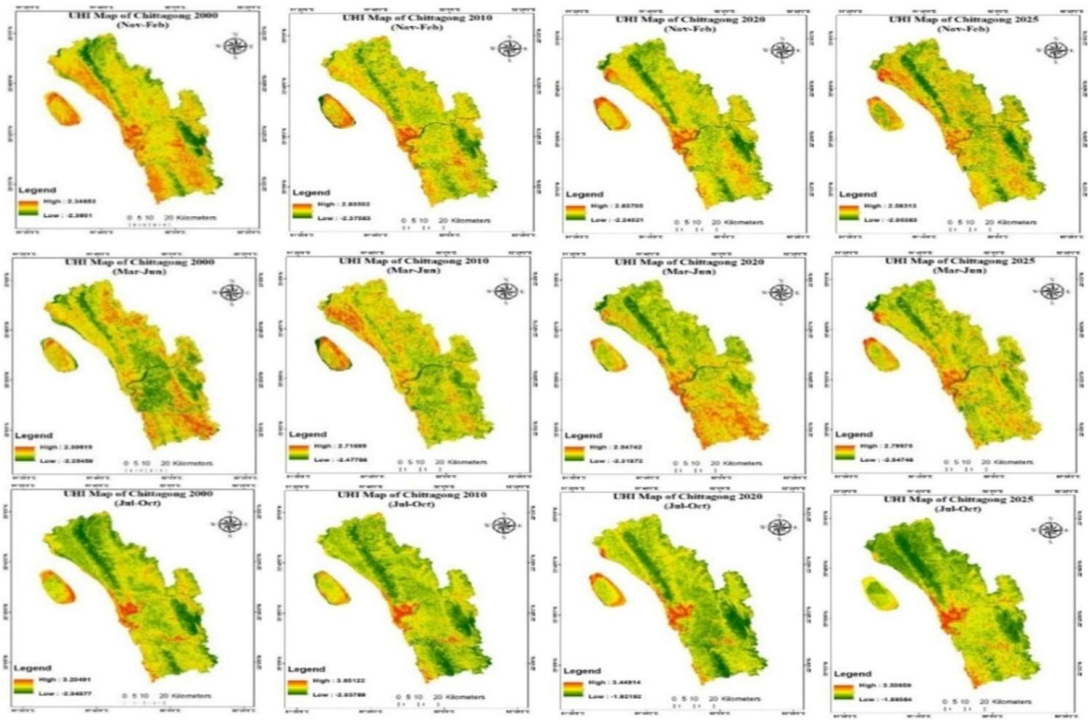

Figure 9: UHI Map of Chittagong during the Winter (Nov-Feb), Transition (Mar-Jun), Monsoon (Jul-Oct) Period (2000,2010,2020 & 2025)

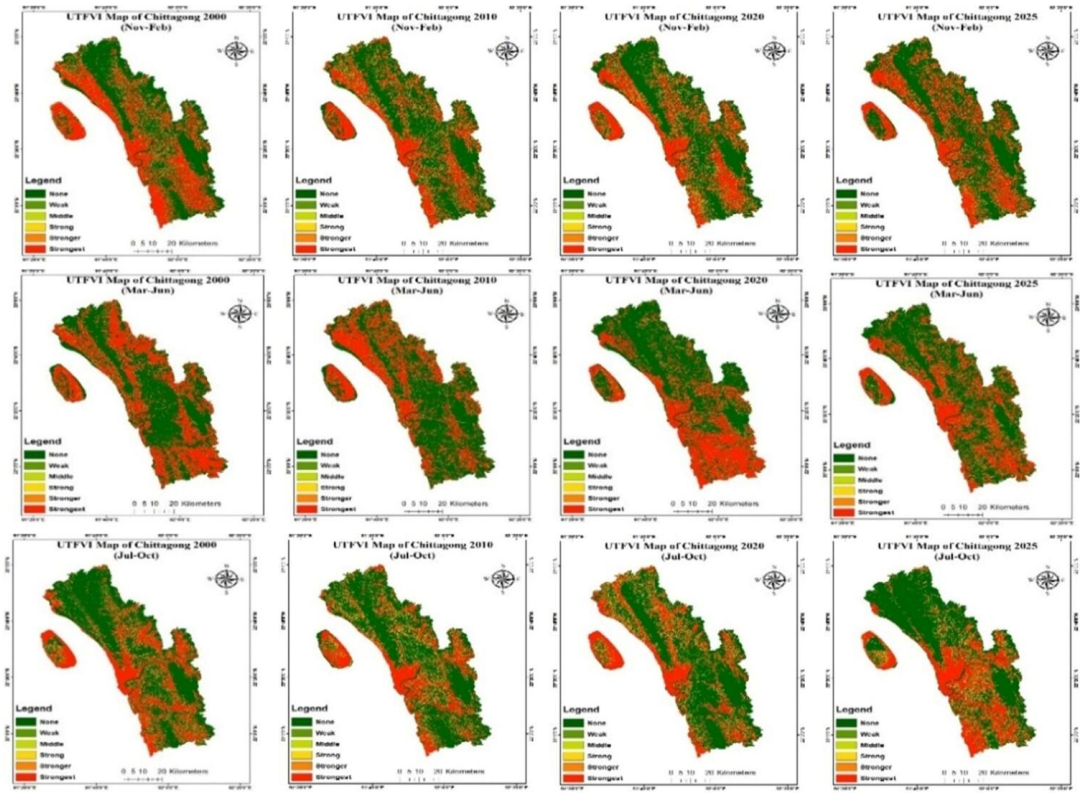

Figure 10: UTFVI Map of Chittagong during the Winter (Nov-Feb), Transition (Mar-Jun), Monsoon (Jul-Oct) Period (2000,2010,2020 & 2025)

E. Spatiotemporal Variations of NDVI, LST, UHI, and UTFVI in Dhaka (2000–2025)

The urban thermal changes were the most significant in Dhaka district. The LULC analysis indicated in **Figure 6** that the area of built-up development grew by more than 100% while the area of agricultural land decreased between 2000 and 2025. Maximum NDVI in

Figure 11 increased moderately from 0.387 to 0.454 in winter and 0.464 to 0.491 in monsoon, whereas the maximum LST in **Figure 12** increased significantly in winter from 30.37°C to 34.62°C and in monsoon from 32.61°C to 39.56°C.

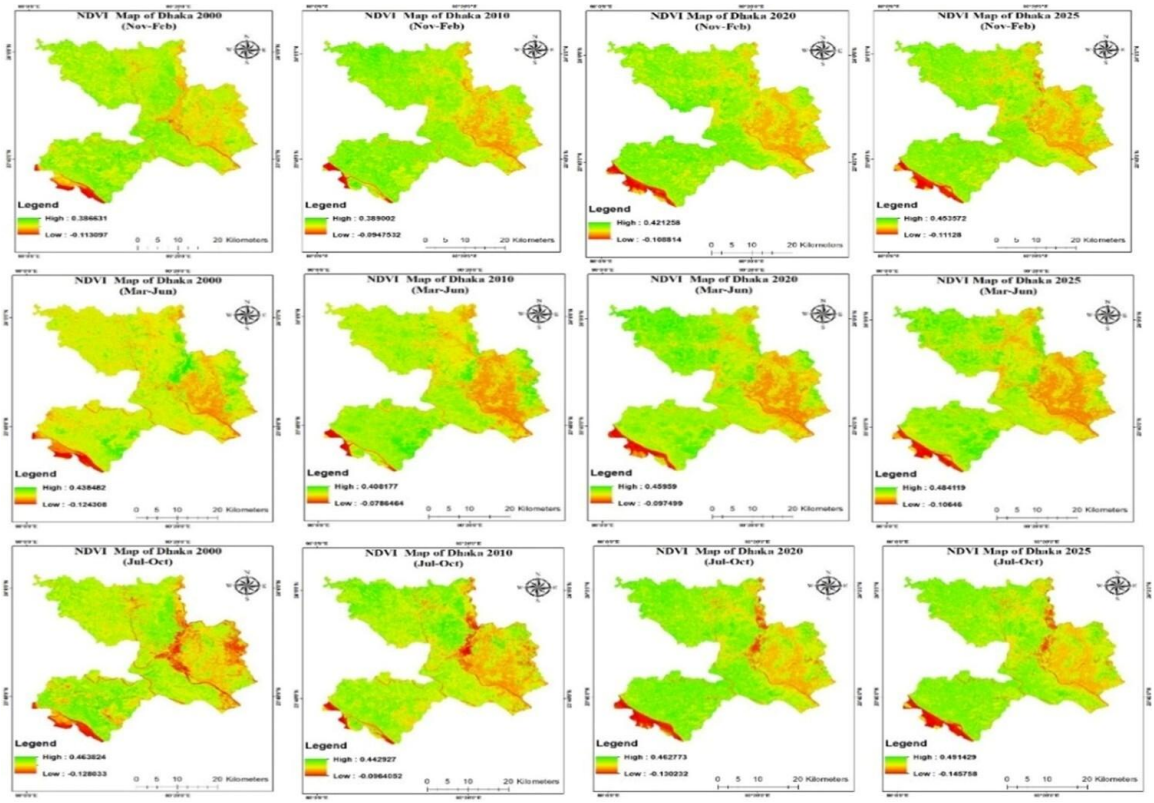

Figure 11: NDVI Map of Dhaka during the Winter (Nov-Feb), Transition (Mar-Jun), Monsoon (Jul-Oct) Period (2000,2010,2020 & 2025)

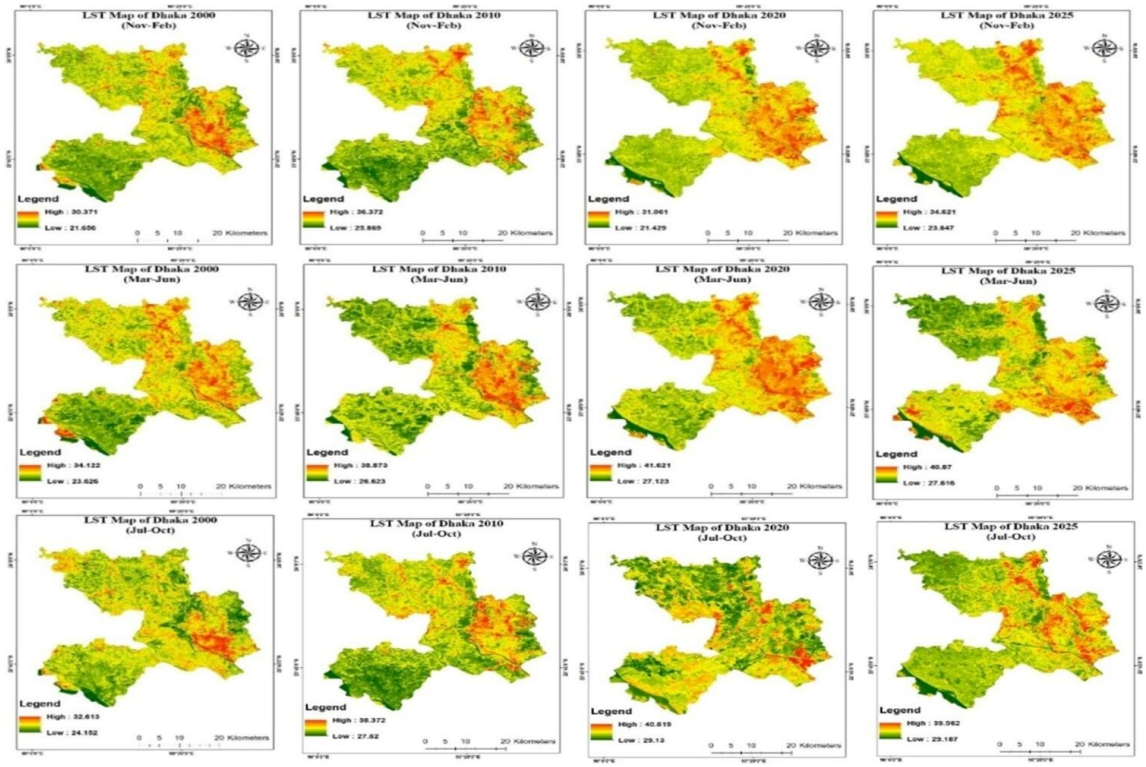

Figure 12: LST Map of Dhaka during the Winter (Nov-Feb), Transition (Mar-Jun), Monsoon (Jul-Oct) Period (2000,2010,2020 & 2025)

The maximum UHI intensity in **Figure 13** was also consistently high, rising from 2.64°C to 2.98°C in winter and from 2.87°C to 3.11°C in the monsoon period. The growth of impervious surfaces and high-density urban fabric has increased the heat accumulation throughout the district. Consequently, greater proportions of strong thermal stress classes are shown in urban core areas as predicted by UTFVI maps in **Figure 14** and represent worsening thermal environmental quality.

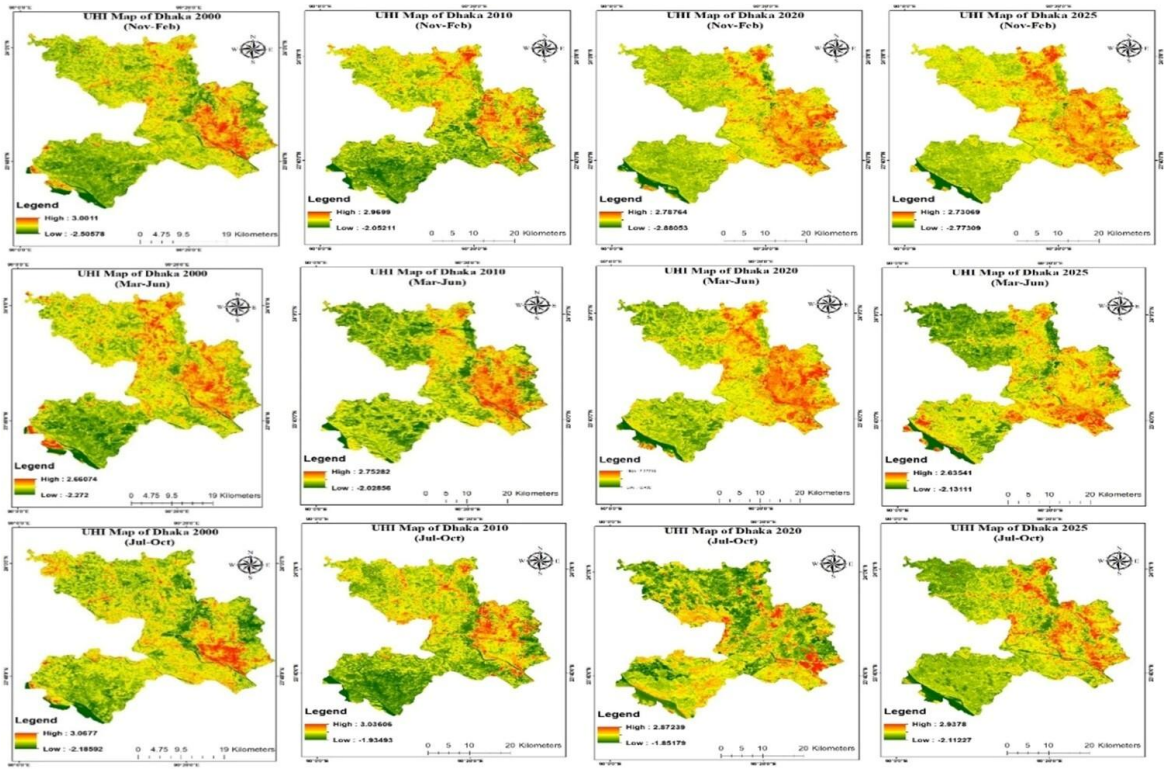

Figure 13: UHI Map of Dhaka during the Winter (Nov-Feb), Transition (Mar-Jun), Monsoon (Jul-Oct) Period (2000,2010,2020 & 2025)

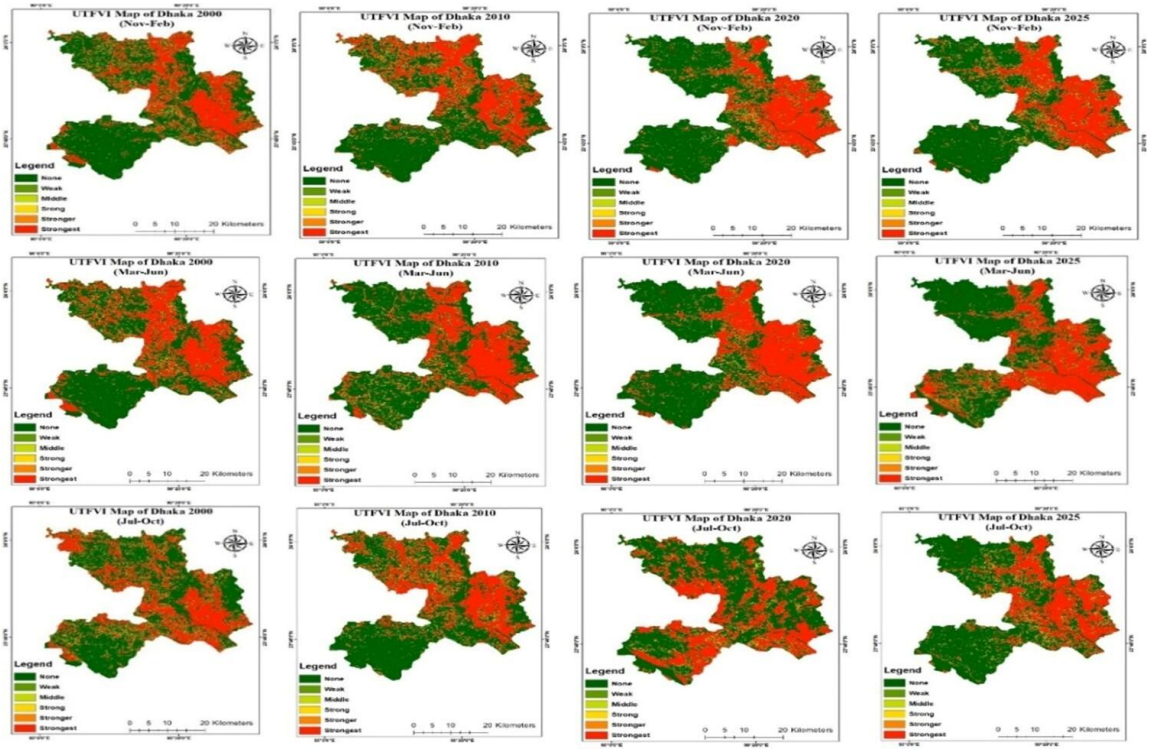

Figure 14: UTFVI Map of Dhaka during the Winter (Nov-Feb), Transition (Mar-Jun), Monsoon (Jul-Oct) Period (2000,2010,2020 & 2025)

The built-up landscape in Dhaka throughout the year meant that there were less seasonal variations than in the other districts. However, during the transition and monsoon seasons, the NDVI was generally high due to the higher levels of rainfall resulting in higher levels of growth for the vegetation. During the transition period, maximum LST in **Figure 12** rose to 40.87°C in 2025, which had minimal pre-monsoon moisture and maximum solar radiation. Despite the decrease in surface temperatures with the monsoon, the urban surface continued to hold heat, resulting in high intensity of UHI and high UTFVI values. This led to high thermal stress levels year-round, especially in the city center.

IV. CONCLUSION

This study examines the spatial and seasonal effects of land use and land cover (LULC) changes on the microclimates of Dhaka and Chittagong, Bangladesh, from 2000 to 2025. Over this 25-year period, both districts experienced significant urban growth. Dhaka's built-up areas increased by nearly 100% to over 106%, leading to a loss of agricultural land and water bodies. Chittagong's urban area expanded by 47% to 53% because of industrial and port development, although its hilly landscape maintained more vegetation. Replacing natural surfaces with hard surfaces severely harmed the thermal environments in both cities. During the peak monsoon, land surface temperatures (LST) rose by 3.75°C in Chittagong and 6.95°C in Dhaka, while the maximum urban heat island (UHI) intensities reached 3.51°C and 3.11°C, respectively. Mapping of the Urban Thermal Field Variance Index (UTFVI) shows the growth of "strong" and "strongest" thermal stress zones in urban centers. Seasonally, the highest thermal peaks happened during the transition (March to June) due to high solar radiation and low moisture. Although monsoon rainfall increased vegetation greenness (NDVI) and temporarily reduced temperatures, this seasonal growth was not enough to offset the ongoing accumulation of urban heat. In conclusion, these results highlight a clear link between rapid urban growth and increasing thermal stress. These findings offer essential data for policymakers to develop climate-smart land-use plans and blue-green infrastructure to decrease UHI effects.

ACKNOWLEDGMENT

We would like to give thanks and show our deep gratitude to the honorable Chairman of SPARRSO for his continuous support and guidance in this research.

REFERENCES

Amani, M., Ghorbanian, A., Ahmadi, S. A., Kakooei, M., Moghimi, A., Mirmazloumi, S. M., Moghaddam, S. H. A., Mahdavi, S., Ghahremanloo, M., Parsian, S., Wu, Q., & Brisco, B. (2020). Google Earth Engine cloud computing platform for remote sensing big data applications: A comprehensive review. IEEE Journal of Selected Topics in Applied Earth Observations and Remote Sensing, 13, 5326–5350. https://doi.org/10.1109/JSTARS.2020.3021052

Avdan, U., & Jovanovska, G. (2016). Algorithm for automated mapping of land surface temperature using LANDSAT 8 satellite data. Journal of Sensors, 2016, 1480307. https://doi.org/10.1155/2016/1480307

Belgiu, M., & Drăguţ, L. (2016). Random forest in remote sensing: A review of applications and future directions. ISPRS Journal of Photogrammetry and Remote Sensing, 114, 24–31. https://doi.org/10.1016/j.isprsjprs.2016.01.011

Bowler, D. E., Buyung-Ali, L., Knight, T. M., & Pullin, A. S. (2010). Urban greening to cool towns and cities: A systematic review of the empirical evidence. Landscape and Urban Planning, 97(3), 147–155. https://doi.org/10.1016/j.landurbplan.2010.05.006

Cao, X., Onishi, A., Chen, J., & Imura, H. (2010). Quantifying the cool island intensity of urban parks using ASTER and IKONOS data. Landscape and Urban Planning, 96(4), 224–231. https://doi.org/10.1016/j.landurbplan.2010.03.008

Chen, X. L., Zhao, H. M., Li, P. X., & Yin, Z. Y. (2006). Remote sensing image-based analysis of the relationship between urban heat island and land use/cover changes. Remote Sensing of Environment, 104(2), 133–146. https://doi.org/10.1016/j.rse.2005.11.016

Drusch, M., Del Bello, U., Carlier, S., Colin, O., Fernandez, V., Gascon, F., Hoersch, B., Isola, C., Laberinti, P., Martimort, P., Meygret, A., Spoto, F., Sy, O., Marchese, F., & Bargellini, P. (2012). Sentinel-2: ESA's optical high-resolution mission for GMES operational services. Remote Sensing of Environment, 120, 25–36. https://doi.org/10.1016/j.rse.2011.11.026

Gorelick, N., Hancher, M., Dixon, M., Ilyushchenko, S., Thau, D., & Moore, R. (2017). Google Earth Engine: Planetary-scale geospatial analysis for everyone. Remote Sensing of Environment, 202, 18–27. https://doi.org/10.1016/j.rse.2017.06.031

Grimm, N. B., Faeth, S. H., Golubiewski, N. E., Redman, C. L., Wu, J., Bai, X., & Briggs, J. M. (2008). Global change and the ecology of cities. Science, 319(5864), 756–760. https://doi.org/10.1126/science.1150195

Hasan, M. M., Islam, A. R. M. T., Badhan, M. A., & Kamruzzaman, M. (2023). Exploring spatiotemporal urban heat island dynamics and its relationship with land use land cover change in Dhaka city, Bangladesh. Environmental Monitoring and Assessment, 195(2), 242. https://doi.org/10.1007/s10661-022-10827-y

He, J., Liu, J., Zhuang, D., Zhang, W., & Liu, M. (2011). Assessing the effect of land use/land cover change on the change of urban heat island intensity. Theoretical and Applied Climatology, 107(1–2), 65–76. https://doi.org/10.1007/s00704-011-0463-z

Iqbal, M. J., & Khan, M. N. (2014). Spatiotemporal assessment of land use/land cover and its impact on land surface temperature of Chittagong city, Bangladesh. Journal of Geographic Information System, 6(6), 628–636. https://doi.org/10.4236/jgis.2014.66052

Islam, M. S., Urmy, S. S., Farjana, N., & Huq, M. E. (2019). Spatiotemporal dynamics of land use land cover change and land surface temperature in Dhaka district, Bangladesh. Ecological Processes, 8(1), 35. https://doi.org/10.1186/s13717-019-0192-3

Islam, M. S., Amin, M. N., & Atiqur Rahman, M. (2021). Dynamics of land use and land cover change and its impacts on the thermal environment of Chittagong, Bangladesh. Remote Sensing Applications: Society and Environment, 22, 100518. https://doi.org/10.1016/j.rsase.2021.100518

Li, J., Song, C., Cao, L., Zhu, F., Meng, X., & Wu, J. (2011). Impacts of landscape structure on surface urban heat islands: A case study of Shanghai, China. Remote Sensing of Environment, 115(12), 3249–3263. https://doi.org/10.1016/j.rse.2011.07.008

Oke, T. R. (1982). The energetic basis of the urban heat island. Quarterly Journal of the Royal Meteorological Society, 108(455), 1–24. https://doi.org/10.1002/qj.49710845502

Patz, J. A., Campbell-Lendrum, D., Holloway, T., & Foley, J. A. (2005). Impact of regional climate change on human health. Nature, 438(7066), 310–317. https://doi.org/10.1038/nature04188

Rana, M. P., Chowdhury, M. S. H., & Islam, M. T. (2021). Urban expansion and its effects on the land surface temperature of Dhaka city: A remote sensing-based approach. Bangladesh Journal of Geography, 1(1), 45–56.

Sobrino, J. A., Jiménez-Muñoz, J. C., & Paolini, L. (2004). Land surface temperature retrieval from LANDSAT TM 5. Remote Sensing of Environment, 90(4), 434–440. https://doi.org/10.1016/j.rse.2004.02.003

UN-Habitat. (2022). World cities report 2022: Envisaging the future of cities. United Nations Human Settlements Programme.

Weng, Q. (2009). Thermal infrared remote sensing for urban climate and environmental studies: Methods, applications, and trends. ISPRS Journal of Photogrammetry and Remote Sensing, 64(4), 335–344. https://doi.org/10.1016/j.isprsjprs.2009.03.007

Weng, Q., Lu, D., & Schubring, J. (2004). Estimation of land surface temperature–vegetation abundance relationship for urban heat island studies. Remote Sensing of Environment, 89(4), 467–483. https://doi.org/10.1016/j.rse.2003.11.005

World Bank. (2023). World development indicators: Urban population. https://data.worldbank.org/indicator/SP.URB.TOTL

Wulder, M. A., Roy, D. P., Radeloff, V. C., Loveland, T. R., Anderson, M. C., Johnson, D. M., Healey, S., Zhu, Z., Scambos, T. A., Pahlevan, N., Hansen, M., Gorelick, N., Crawford, C. J., Masek, J. G., Hermosilla, T., White, J. C., Belward, A. S., Schaaf, C., Sellers, P., … Cook, B. D. (2022). Fifty years of Landsat science and impacts. Remote Sensing of Environment, 280, 113195. https://doi.org/10.1016/j.rse.2022.113195

Zhao, L., Lee, X., Smith, R. B., & Oleson, K. (2014). Strong contributions of local background climate to urban heat islands. Nature, 511(7508), 216–219. https://doi.org/10.1038/nature13462

Zhou, W., Huang, G., & Cadenasso, M. L. (2011). Does spatial configuration matter? Understanding the effects of land cover pattern on land surface temperature in urban landscapes. Landscape and Urban Planning, 102(1), 54–63. https://doi.org/10.1016/j.landurbplan.2011.03.009

AUTHORS

First Author – Md. Farid Uddin, Scientific Officer, SPARRSO, E-mail: farid.uddin@sparrso.gov.bd

Second Author – Mohammad Shahidul Islam, Principal Scientific Officer, SPARRSO, E-mail: shohidul@sparrso.gov.bd

Third Author – Fatema Afnan Chowdhury, Research Fellow, SPARRSO, E-mail: fatemachy20@gmail.com.

Fourth Author – Md. Mahadi Hasan Seyam, Research Fellow, SPARRSO, E-mail: seyamenv46ju@gmail.com.

Fifth Author – Adib Mahmud, Research Fellow, SPARRSO, E-mail: adibmahmud308@gmail.com

Sixth Author – Ishpiya Mahreen Chowdhury, Research Fellow, SPARRSO, E-mail: ishpiya.mahreen@gmail.com

Correspondence Author – Md. Farid Uddin, Scientific Officer, SPARRSO, farid.uddin@sparrso.gov.bd